Supporting Information

Synthesis of a Stable Benzoxazole Gel from an Imine Gel for Adsorption and Catalysis

Yu Xin, Junxing Chen, Zujin Yang and Jianyong Zhang*

Sun Yat-Sen University, MOE Laboratory of Polymeric Composite and Functional Materials, School of Materials Science and Engineering, School of Chemical Engineering and Technology, Guangzhou 510275, China.

Corresponding Author

* zhjyong@mail.sysu.edu.cn (J. Z.).

CONTENTS

1. Experimental methods
2. Determined kinetic parameters for the adsorption of Pd^{2+} and adsorption uptake of Pd^{2+} determined by UV-vis spectroscopy
3. Adsorption of Pd(II) by various adsorbents and reduction of Cr(VI) by various nanocatalysts
4. Linearly-fitted calibration curve of Pd(II) and $K_2Cr_2O_7$
5. FT-IR spectra
6. QSDFT pore size distribution
7. Chemical stability
8. Thermogravimetric (TG) profiles
9. Kinetic models for Pd^{2+} adsorption
10. XPS spectra
11. Oscillatory rheological measurements
12. Pseudo-first-order kinetic model for reduction of Cr(VI)
13. Reusability performance

Experimental Methods

Chemicals and solvents were obtained from commercial sources and used as received without further purification unless otherwise stated. 4-{2,2-bis[(4-formylphenoxy)methyl]-3-(4-formylphenoxy)propoxy}benzaldehyde (A4) was synthesized according to the reported method.[35] ^{1}H NMR was performed on Bruker advance III 400MHz. Solid-State NMR Measurements were carried out at room temperature on a Bruker Avance 400 MHz spectrometer. UV-vis spectra were carried out on RIGOL Ultra-3600 UV spectrophotometer. FT-IR was carried out on PerkinElmer Frontier FT-IR using KBr pellets. Rheological measurements were carried out on a HAAKE MARS(III) rheometer at 298 K. N_2 adsorption measurements were performed using a Quantachrome Autosorb-iQ2analyzer. XRD measurement was performed on D-MAX 2200 VPC instrument. TEM was conducted on a FEI Tecnai G2 Spirit 120 kV transmission electron microscope. For TEM measurement, the material was dispersed in EtOH with the aid of sonication, and then mounted on a carbon coated copper grid. SEM was conducted on HITACHI SU8010 scanning electron microscope. Prior to SEM measurements, the material was dispersed in EtOH with the aid of sonication, and then deposited on aluminium foil. Thermogravimetric analyses were carried out in a nitrogen stream using Netzsch STA 449F3-jupiter thermogravimetric-differential scanning calorimetry (TG-DSC) analyzer with a heating rate of 10 °C min^{-1}. Metal (Pd) analyses were performed by using an Inductively Coupled Plasma-atomic Emission Spectrometer (ICP-OES; Optima 8300, USA, Perkin Elmer). X-ray photoelectron spectroscopy (XPS) was tested on Nexsa Thermo ESCALAB 250Xi instrument with an Al Kα X-ray source (Thermo Fisher). Contact angle tests of aerogel samples were tested on Drop Shape Analyzer-DSA30 (RKRÜSS GmbH, Germany). Rheological measurements were performed on a HAAKE MARS(III) rheometer at 298 K. The diameter of upper plate is 20 mm, and the distance between the lower and upper plates is 2.5 mm for the tests. The concentrations of metal Pd(II) and Cr(VI) ions were determined by Perkin Elmer inductively coupled plasma-atomic emission spectrometer (ICP-OES; Optima 8300, USA) and RIGOL Ultra-3600 UV spectrophotometer.

Table S1. Determined kinetic parameters for the adsorption of Pd^{2+}.

Pseudo-first order			Elovich's equation			Pseudo-second order		
q_e /mg g^{-1}	k /min^{-1}	R^2	a /mg g^{-1} min^{-1}	1/b /mg g^{-1}	R^2	k' /g mg^{-1} min^{-1}	q_e /mg g^{-1}	R^2
239.22	8.63×10^{-3}	0.99	20.11	41.01	0.96	7.5×10^{-5}	257.73	0.99

Table S2. Adsorption of Pd(II) by various adsorbents.

Entry	Adsorbent for Pd(II)	Contact time /h	pH	Adsorption capacity /mg g^{-1}	Ref.
1	Activated carbon	4.5	<1	27.00	S1
2	Chitosan coated activated carbon	3.3	2	43.48	S2
3	HMBA@mesoporous inorganic silica monoliths	2	3.5	172.53	S3
4	Modified carbon nanotube	\	6	15.6	S4
5	THTB@mesoporous silica	3	3.5	171.65	S5
6	Commercial tris(2-aminoethyl) amine polystyrene polymer beads	24	1	206.93	S6
7	Pyridyltriazol functionalized zirconium MOF	0.08	4.5	294.10	S7
8	Glutaraldehyde cross-linked chitosan resin	5	8	166.67	S8
9	Glutaraldehyde cross-linked chitosan	24	2	180.00	S9
10	Crosslinked chitosan resin	4	2	120.4	S10
11	MFT resin	\	4	15.3	S11
12	Pyridine based polymer	6	1	191.6	S12
13	Poly (4-vinylpyridine) resins	48	1	43	S13
14	Lysine modified crosslinked chitosan	4	2	109.47	S14
15	Polyamine functionalized polystyrene	0.5	<1	4.3	S15
16	N-substituted 2-(diphenylthiophosphoryl)acetamides	1	<1	52.77	S16
17	Polyethylenimine/polyvinyl chloride crosslinked adsorbent	1	1	146.03	S17
18	A4B2-Benzoxazole gel	24	3	250.00	This work

Table S3. Adsorption uptake of Pd^{2+} at room temperature determined by UV-vis spectroscopy.

Entry[a]	Abs.[b] (t = 0 d)	Abs.[b] (t = 4 d)	Amount of Pd^{2+} in gel/μmol
1	0.963	0.594	19
2	0.950	0.593	19
3	0.958	0.549	21
4	0.962	0.537	22
5	0.965	0.561	21
6	0.967	0.543	22

[a] 10 mL $PdCl_2$ solution (5 mmol L^{-1}) was added to 1 mL A4B2-benzoxazole gel prepared from 0.02 mmol A4. [b] Absorbance at λ ~ 425 nm.

Various nanoparticles such as palladium nanoparticles (Pd NPs), sulfur nanoparticles (S NPs), NiO nanoparticles (NiO NPs), iron nanoparticles (Fe NPs), ZnO nanorods and TiO_2 nanoparticles (TiO_2 NPs) have been used as catalysts for the reduction and removal of Cr(VI) in recent years. The first-order reaction rate constant and turnover frequency (TOF) of the nanomaterials for reduction of Cr(VI) are listed in Table S4. The reduction of Cr(VI) catalyzed by Pd@A4B2-benzoxazole gel can be completed within 60 min with a rate constant of 0.0377 min^{-1}, and the TOF is about 6.37×10^{-5} mol g^{-1} min^{-1}. The activity is comparable with biosynthesis Pd NPs (0.0971 min^{-1}), and higher than magnetic mesoporous carbon-doped Pd NPs (0.017 min^{-1}) and some metal nanocatalysts such as NiO nanostructure (2.50×10^{-6} mol g^{-1} min^{-1}), nanoscale zero-valent iron (6.087×10^{-6} mol g^{-1} min^{-1}), ZnO nanorods (3.08×10^{-6} mol g^{-1} min^{-1}) and TiO_2 nanoparticles (9.63×10^{-6} mol g^{-1} min^{-1}).

Table S4. Reduction of Cr(VI) by various nanocatalysts.

Entry	Nanocatalyst	Rate constant /min^{-1}	TOF /mol g^{-1} min^{-1}	Ref.
1	Pd@Pro-ESM	0.133	0.808×10^{-5}	S18
2	Pd/γ-Al_2O_3	0.085	\	S19
3	Pd-TMV	0.25	0.657×10^{-3}	S20
4	Biogenic Pd(0) nanoparticles	0.0971	\	S21
5	Cobalt nanoparticles supported on graphene	0.474	0.46×10^{-3}	S22
6	Magnetic mesoporous carbon-doped Pd NPs	0.017	\	S23
7	Nanoscale zero-valent iron supported on mesoporous silica	0.017	6.087×10^{-6}	S24
8	Sulfur nanoparticles	0.027	1.04×10^{-2}	S25
9	ZnO nanorods	0.016	3.08×10^{-6}	S26
10	TiO_2 nanoparticles	0.035	9.63×10^{-6}	S27
11	NiO nanostructure	0.0026	2.50×10^{-6}	S28
12	Pd@A4B2-benzoxazole gel	0.0377	6.37×10^{-5}	This work

References

S1 Kasaini, E.; Goto, M.; Furusaki, S. Selective Separation of Pd(II), Rh(III), and Ru(III) Ions from a Mixed Chloride Solution Using Activated Carbon Pellets. *Sep. Sci. Technol.* **2000**, *35*, 1307-1327.

S2 Sharififard, H.; Ashtiani, F. Z.; Soleimani, M. Adsorption of Palladium and Platinum from Aqueous Solutions by Chitosan and Activated Carbon Coated with Chitosan. *Asia-Pac. J. Chem. Eng.* **2013**, *8*, 384-395.

S3 Awual, M. R.; Rahman, I. M. M.; Yaita, T.; Khaleque, M. A.; Ferdows, M. pH Dependent Cu(II) and Pd(II) Ions Detection and Removal from Aqueous Media by an Efficient Mesoporous Adsorbent. *Chem. Eng. J.* **2014**, *236*, 100-109.

S4 Yuan, C.; Zhang, Y.; Wang, S.; Chang, A. Separation and Preconcentration of Palladium Using Modified Multi-Walled Carbon Nanotube without Chelating Agent. *Microchim. Acta* **2011**, *173*, 361-367.

S5 Awuala, M. R.; Hasan, M. M.; Naushad, M.; Shiwaku, H.; Yaita, T. Preparation of new class composite adsorbent for enhanced palladium(II) detection and recovery. *Sensor Actuat. B-Chem.* **2015**, *209*, 790-797.

S6 Sayın, M.; Can, M.; İmamoğlu, M. Adsorption of Pd(II) and Au(III) Ions by Commercial Tris(2-Aminoethyl) Amine Polystyrene Polymer Beads. *J. Chem. Eng. Data* **2021**, *66*, 1132-1143.

S7 Daliran, S.; Ghazagh-Miri, M.; Oveisi, A. R.; Khajeh, M.; Navalón, S.; Âlvaro, M.; Ghaffari-Moghaddam, M.; Delarami, H. S.; García, H. A Pyridyltriazol Functionalized Zirconium Metal-Organic Framework for Selective and Highly Efficient Adsorption of Palladium. *ACS Appl. Mater. Interfaces* **2020**, *12*, 25221-25232.

S8 Nagireddi, S.; Katiyar, V.; Uppaluri, R. Pd(II) adsorption characteristics of glutaraldehyde cross-linked chitosan copolymer resin. *Int. J. Biol. Macromol.* **2017**, *94*, 72-84.

S9 Ruiz, M.; Sastre, A. M.; Guibal, E. Palladium Sorption on Glutaraldehyde-Crosslinked Chitosan. *React. Funct. Polym.* **2000**, *45*, 155-173.

S10 Ramesh, A.; Hasegawa, H.; Sugimoto, W.; Maki, T.; Ueda, K. Adsorption of Gold(III), Platinum(IV) and Plladium(II) onto Gycine Mdified Cosslinked Citosan Rsin. *Bioresour. Technol.* **2008**, *99*, 3801-3809.

S11 Brinci, E.; Gülfen, M.; Aydin, A.O.; Separation and Recovery of Palladium(II) from Base Metal ions by Melamine-Formaldehyde-Thiourea (MFT) Chelating Resin. *Hydrometallurgy* **2009**, *95*, 15-21.

S12 Kumar, V. V.; Kumar, C. R.; Suresh, A.; Jayalakshmi, S.; Mudali, U. K.; Sivaraman, N. Evaluation of Polybenzimidazole-based Polymers for the Removal of Uranium, Thorium and Palladium from Aqueous Medium. *Roy. Soc. Open Sci.* **2018**, *5*, 171701.

S13 Jermakowicz-Bartkowiak, D.; Kolarz, B. N. Poly(4-vinylpyridine) Resins towards Perrhenate Sorption and Desorption. *React. Funct. Polym.* **2011**, *71*, 95-103.

S14 Fujiwara, K.; Ramesh, A.; Maki, T.; Hasegawa, H.; Ueda, K. Adsorption of Platinum(IV), Palladium (II) and Gold (III) from Aqueous Solutions onto l-Lysine Modified Crosslinked Chitosan Resin. *J. Hazard. Mater.* **2007**, *146*, 39-50.

S15 Fayemi, O. E.; Ogunlaja, A. S.; Kempgens, P. F. M.; Antunes, E.; Torto, N.; Nyokong, T.; Tshentu, Z. R. Adsorption and Separation of Platinum and Palladium by Polyamine Functionalized Polystyrene-Based Beads and Nanofibers. *Miner. Eng.* **2013**, *53*,

256-265.
S16 Turanov, A. N.; Karandashev, V.; Artyushin, O. I.; Sharova, E. V.; Genkina, G. K. Adsorption of Palladium(II) from Hydrochloric Acid Solutions Using Polymeric Resins Impregnated with Novel N-Substituted 2-(diphenylthiophosphoryl)acetamides. *Sep. Purif. Technol.* **2017**, *187*, 355-364.
S17 Choi, H. A.; Park, H. N.; Won, S. W. A Reusable Adsorbent Polyethylenimine/polyvinyl Chloride Crosslinked Fiber for Pd(II) Recovery from Acidic Solutions. *J. Environ. Manage.* **2017**, *204*, 200-206.
S18 Liang, M.; Su, R.; Qi, W.; Zhang, Y.; Huang, R.; Yu, Y.; Wang, L. He, Z. Reduction of Hexavalent Chromium Using Recyclable Pt/Pd Nanoparticles Immobilized on Procyanidin-Grafted Eggshell Membrane. *Ind. Eng. Chem. Res*. **2014**, *53*, 13635-13643
S19 Dandapat, A.; Jana, D.; De, G. Pd Nanoparticles Supported Mesoporous γ-Al_2O_3 Film as a Reusable Catalyst for Reduction of Toxic CrVI to CrIII in Aqueous Solution. *Appl. Catal. A* **2011**, *396*, 34-39.
S20 Yang, C.; Yi, H. Facile Approaches to Control Catalytic Activity of Viral-Templated Palladium Nanocatalysts for Dichromate Reduction. *Biochem. Eng. J.* **2010**, *52*, 160-167.
S21 Tripathi, R. M.; Chung, S. J. Reclamation of Hexavalent Chromium Using Catalytic Activity of Highly Recyclable Biogenic Pd(0) Nanoparticles. *Sci Rep.* **2020**, *10*, 640.
S22 Xu, T.; Xue, J.; Zhang, X.; He, G.; Chen, H. Ultrafine Cobalt Nanoparticles Supported on Reduced Graphene Oxide: Efficient Catalyst for Fast Reduction of Hexavalent Chromium at Room Temperature. *Appl. Surf. Sci.* **2017**, *402*, 294-300.
S23 Li, S.; Tang, L.; Zeng, G.; Wang, J.; Deng, Y.; Wang, J.; Xie, Z.; Zhou, Y. Catalytic Reduction of Hexavalent Chromium by a Novel Nitrogen-Functionalized Magnetic Ordered Mesoporous Carbon Doped with Pd Nanoparticles, *Environ. Sci. Pollut. Res.* **2016**, *23*, 22027-22036.
S24 Petala, E.; Dimos, K.; Douvalis, A.; Bakas, T.; Tucek, J.; Zbořil, R.; Karakassides, M. A. Nanoscale Zero-Valent Iron Supported on Mesoporous Silica: Characterization and Reactivity for Cr(VI) Removal from Aqueous Solution. *J. Hazard. Mater.* **2013**, *261*, 295-306.
S25 Tripathia, R. M.; Rao, R. P.; Tsuzuki, T. Green Synthesis of sulfur Nanoparticles and Evaluation of their Catalytic Detoxification of Hexavalent Chromium in Water. *RSC Adv.* **2018**, *8*, 36345-36352.
S26 Shirzad-Siboni, M.; Farrokhi, M.; Soltani, R. D. C.; Khataee, A.; Tajassosi, S. Photocatalytic Reduction of Hexavalent Chromium over ZnO Nanorods Immobilized on Kaolin. *Ind. Eng. Chem. Res.* **2014**, *53*, 1079-1087.
S27 Wang, X.; Pehkonen, S. O.; Ray, A. K. Removal of Aqueous Cr(VI) by a Combination of Photocatalytic Reduction and Coprecipitation. *Ind. Eng. Chem. Res.* **2004**, *43*, 1665-1672.
S28 Qamar, M.; Gondal, M. A.; Yamani, Z. H. Synthesis of Nanostructured NiO and its Application in Laser-Induced Photocatalytic Reduction of Cr (VI) from Water. *J. Mol. Catal. A: Chem.* **2011**, *341*, 83-88.

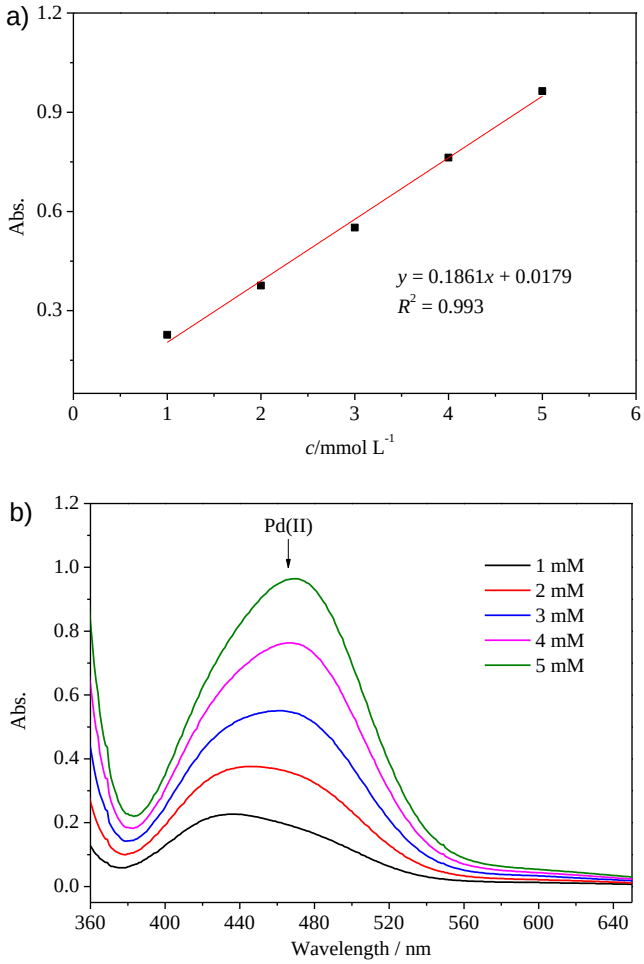

Figure S1. a) Linearly-fitted calibration curve of Pd(II) in a concentration range from 1 to 5 mmol L^{-1}, and b) UV spectra of $PdCl_2$ solution from 1 to 5 mmol L^{-1}.

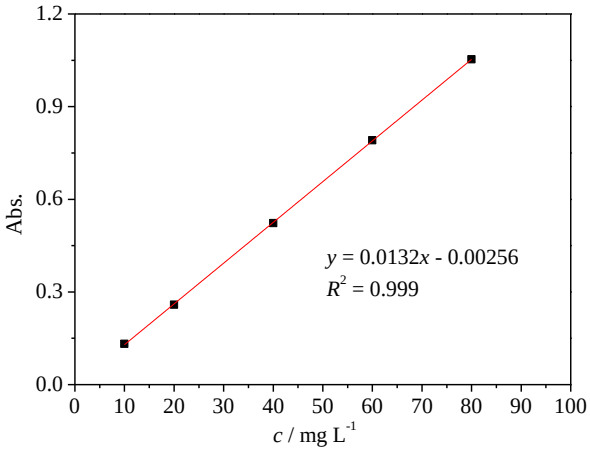

Figure S2. Linearly-fitted calibration curve of $K_2Cr_2O_7$ in concentration range from 10 to 80 mg L^{-1}.

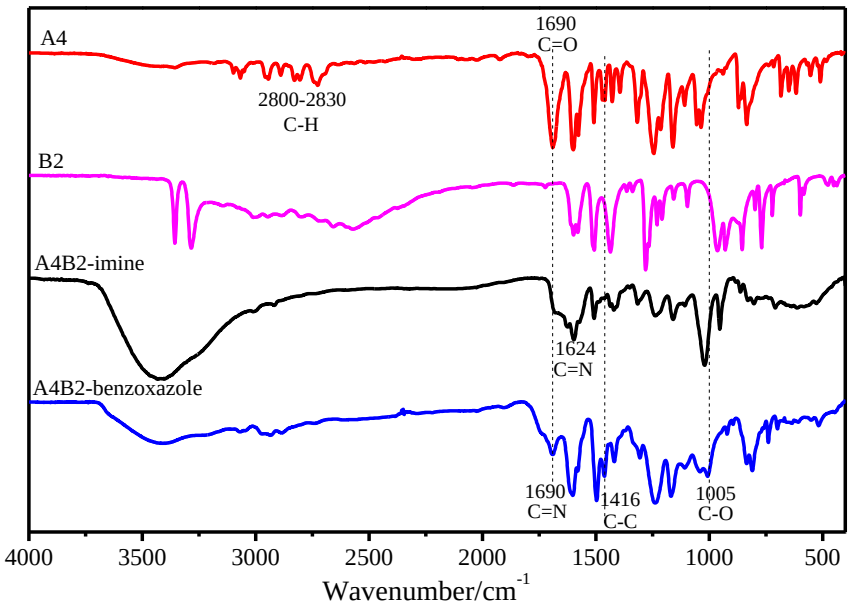

Figure S3. FT-IR spectra of A4B2-benzoxazole xerogel, A4B2-imine xerogel, A4 and B2.

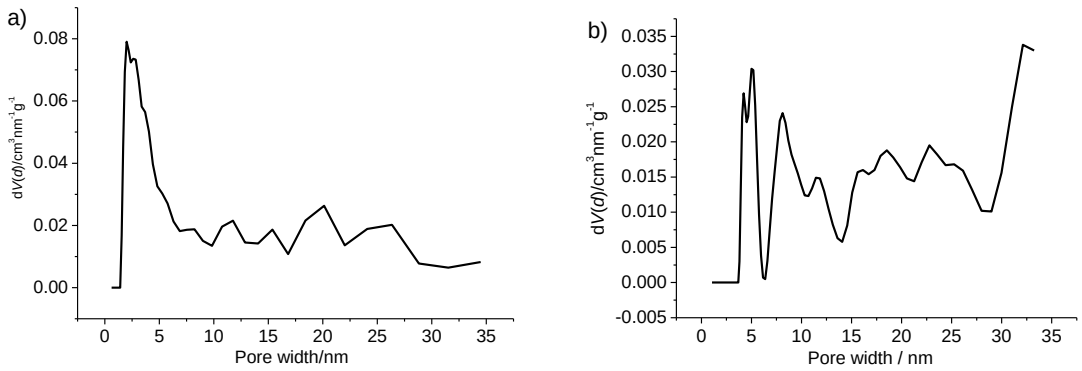

Figure S4. QSDFT pore size distribution (Model: N_2 at 77 K on carbon (cylindr. pores, QSDFT adsorption branch)), a) A4B2-imine aerogel and b) A4B2-benzoxazole aerogel.

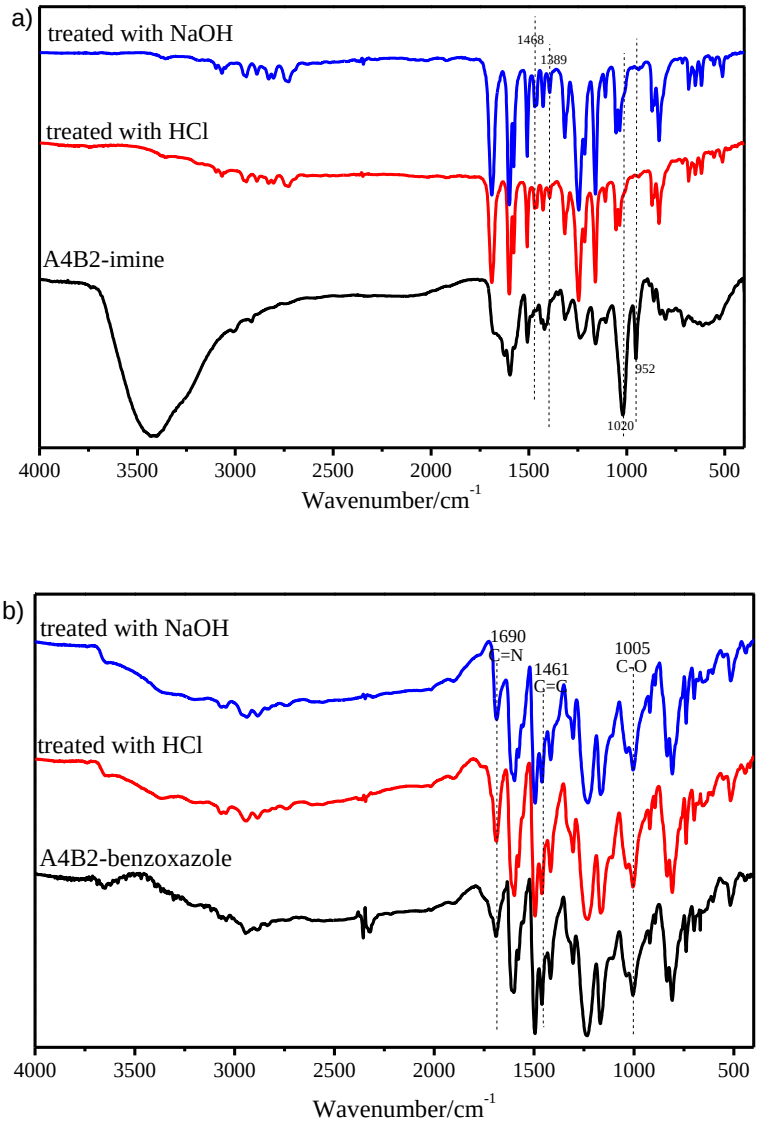

Figure S5. a) FT-IR spectra of A4B2-imine gel, treated in 9 mol L^{-1} HCl for 3 d and treated in 9 mol L^{-1} NaOH solution for 3 d, and b) FT-IR spectra of A4B2-benzoxazole gel, treated in 9 mol L^{-1} HCl for 3 d and treated in 9 mol L^{-1} NaOH solution for 3 d.

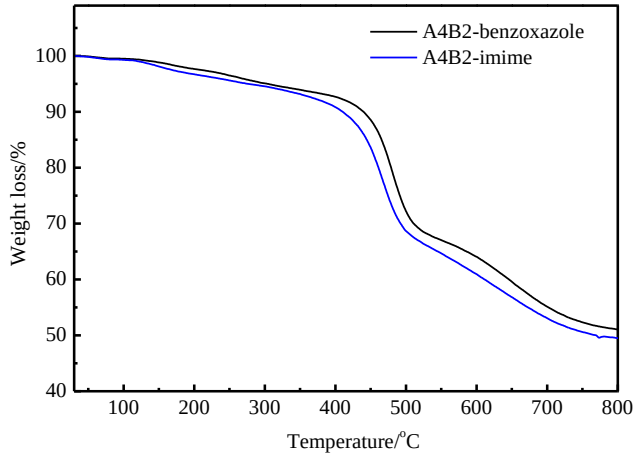

Figure S6. Thermogravimetric (TG) profiles of A4B2-imine and A4B2-benzoxazole aerogels.

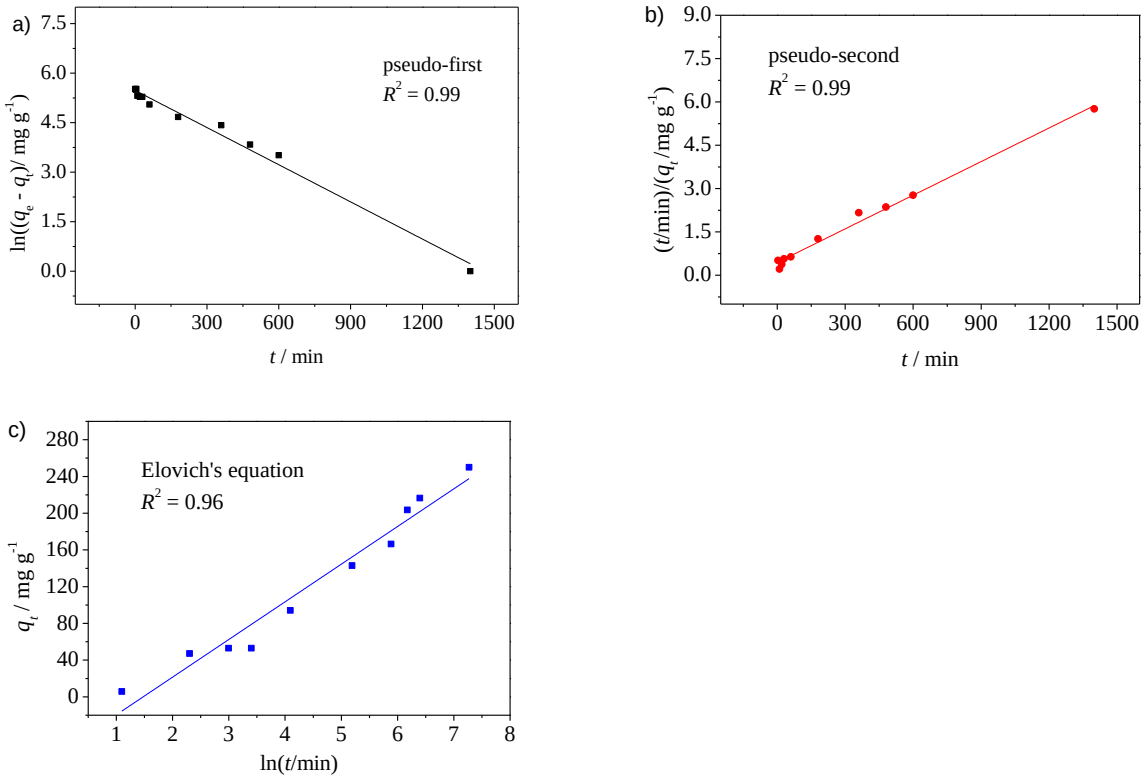

Figure S7. a) Pseudo-first model, b) pseudo-second model and c) Elovich model for Pd^{2+} adsorption onto A4B2-benzoxazole gel at 25 °C, pH = 3.

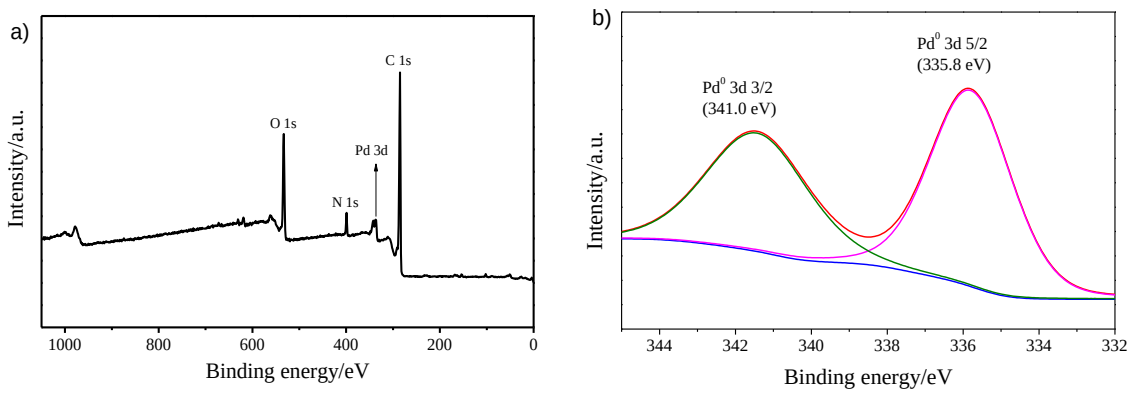

Figure S8. a) XPS survey and b) Pd 3d spectra of Pd@A4B2-benzoxazole xerogel (atomic% Pd 1.13%).

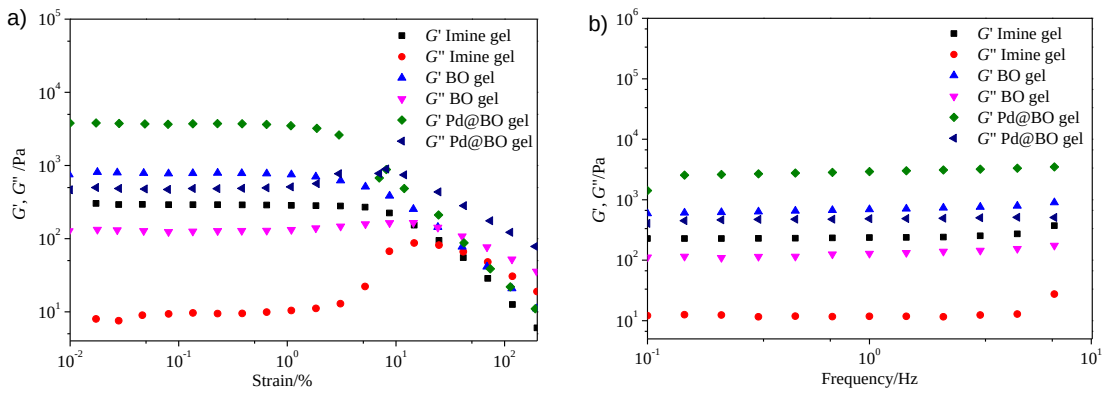

Figure S9. Oscillatory rheological measurements for A4B2-imine, A4B2-benzoxazole and Pd@A4B2-benzoxazole gels, a) strain dependence at 1 Hz and b) frequency sweep experiments performed at 1% strain amplitude.

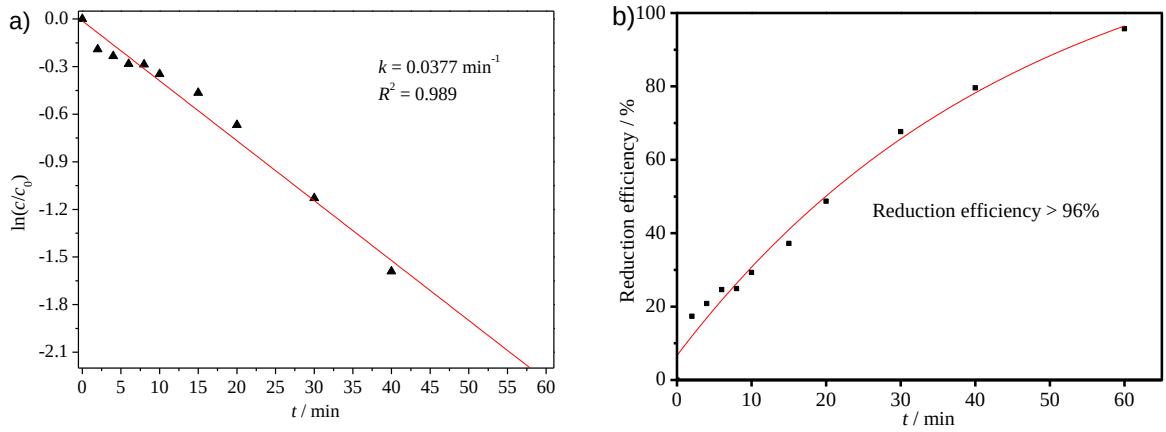

Figure S10. a) Pseudo-first-order kinetic model of ln(c/c_0) versus time, and b) reduction efficiency (%) versus time for reduction of Cr(VI).

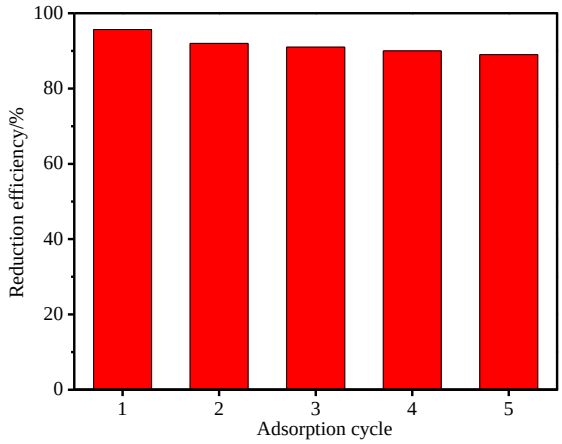

Figure S11. Reusability performance of Pd@A4B2-benzoxazole gel for reduction of Cr(VI).